N72 20212

SEMIANNUAL STATUS REPORT

National Aeronautics and Space Administration

Grant NGL 22-009-337

covering the period

August 16, 1971 - February 15, 1972

Submitted by: Paul Penfield, Jr.

February 15, 1972

MASSACHUSETTS INSTITUTE OF TECHNOLOGY
Research Laboratory of Electronics
Cambridge, Massachusetts 02139

SUMMARY OF RESEARCH

Avalanche Diodes for the Generation of Coherent Radiation

This is a Semiannual Progress Report for the NASA contract covered by Professor Penfield and Professor Steinbrecher and relates work completed during the past period.

During the past report period research was completed and a paper prepared for publication describing the nearly linear properties of an avalanche-diode operating as a small signal amplifier. The nearly-linear model that is presented in the publication was derived from physical electronics, agrees very well with measurement, and predicts within a few dB the one dB compression point and third-order intercepts to be expected in an amplifier built with a particular device. All of the model parameters may be obtained by simple measurement. A preprint of this publication is included as part of this report.

The Josephson junction has many interesting high-frequency properties and, possibly, considerable microwave potential as a low-noise amplifier. During the past period our efforts regarding Josephson junctions were directed toward estimating the requirements in facilities and personnel in order to begin manufacturing Josephson junctions in the laboratory for experimental purposes. A decision on whether to do research on the microwave applications of Josephson junctions awaits the outcome of this initial investigation.

Two other devices were studied. These are the PIN diode and the MSM diode. We are interested in developing a nonlinear model for the PIN diode that can be used to predict the fundamental limit on intermodulation distortion created by the PIN diode in switching applications. The MSM diode is a microwave negative resistance device that is very similar in structure to a transistor with the base lead open. It behaves like an avalanche diode in that a negative resistance appears across the terminals

of the device when carriers are injected into the depleted region.

The MSM diode differs from the avalanche diode in one very important respect : in the avalanche device injected carriers are formed by the avalanche process, whereas in the MSM diode injected carriers come from "punch-through" which results from complete depletion of the drift region of the diode, as in the case of a transistor when punch through occurs. This means that as an amplifier the MSM diode should have a much lower noise figure than the 18 dB experienced with avalanching devices. In fact, it is expected that the MSM diode may have a noise figure as low as a few dB at frequencies of 4 or 5 gigahertz.

During the next period we will concentrate heavily on the MSM diode and on completing the nonlinear models for the PIN diode.

Circuit Model for Characterizing the Nearly Linear Behavior of Avalanche Diodes in Amplifier Circuits

DEAN F. PETERSON, Member, IEEE,
and DONALD H. STEINBRECHER, Member, IEEE

Abstract — A nonlinear circuit model for avalanche diodes is proposed. The model was derived by assuming that the bias dependence of the elements in a known small-signal equivalent-circuit model for existing diodes arises in a manner consistent with the theory of an idealized "Read-type" device. The model contains a nonlinear R-L branch, a controlled source, and a linear depletion capacitance. The model is used in the nearly linear sense to predict intermodulation distortion and gain compression in avalanche diode amplifiers. Computed results for amplifiers with existing diodes are shown to be in good agreement with experiment.

I. INTRODUCTION

Nonlinear or "nearly linear" circuit models for avalanche diodes, if easily obtained, would be useful for predicting performance limitations in avalanche diode amplifiers which are caused by device nonlinearities. We propose a nonlinear circuit model for an avalanche diode which can be inferred from small-signal or incremental device characterization. For incremental signals, the model reduces to that presented by Steinbrecher and Peterson [1] containing four lumped, bias-dependent elements. The model has a nonlinear R-L branch in parallel with a controlled source and linear capacitance.

The nonlinear terminal equations determined by the model agree with those presented by Evans [2] if one degree of freedom is removed. This model was derived by considering the bias dependence of the elements in the small-signal model [1] in conjunction with a nonlinear theory for a Read type of structure. The nonlinear theory, similar to that of Evans [2], is reviewed in Section III. A nonlinear model for an existing device is presented in Section IV.

In Section V we use the proposed model for nonlinearity to determine intermodulation distortion and gain compression in avalanche diode amplifiers, which are then compared with experimental results on characterized diodes. The results indicate that the nonlinear model may be useful in determining some performance limitations on nonlinear avalanche diode circuits.

II. SMALL-SIGNAL MODEL

The small-signal lumped-element circuit model for the avalanche diode in this analysis, shown in Fig. 1, is that presented by Steinbrecher and Peterson [1]. The model was derived initially by fitting a generalized admittance with four degrees of freedom to measured incremental admittance data taken on X-band avalanche diodes. The elements in the model are generally bias-dependent as indicated in Fig. 1, and this dependence can usually be approximated as

$$L_o(I_D) \cong \frac{\text{const.}}{I_D} = \frac{\lambda}{I_D} \tag{1}$$

$$G_o(I_D) \cong \text{const} \cdot I_D = \gamma I_D \tag{2}$$

$$R_o(I_D) \cong \text{const} = R_o, \tag{3}$$

where I_D represents diode bias current.

The problem is now to determine whether this small-signal model could be derived from the linearization of a nonlinear equivalent circuit model which would represent, to an extent, actual device nonlinearities. If the bias current I_D is regarded as a total static current existing at the terminals of the model in Fig. 1, then one might regard the element bias dependence as caused by linearization of nonlinear circuit elements in the region of static operating points. Extension to large signals would not be clear however, since the elements would depend on total static circuit current and not on individual branch currents.

To determine how the small-signal model might be extended to a first-order nonlinear model, an idealized Read-type structure is analyzed for nonincremental signals in a manner similar to that of Evans [2]. A nonlinear circuit model is developed for this device and shown to have small-signal characteristics and element bias variations which are quite similar to those of the empirical model. Using this result, a first-order nonlinear model is proposed for existing diodes.

III. A NONLINEAR CIRCUIT MODEL FOR AN IDEALIZED READ-TYPE DIODE STRUCTURE

The type of diode used in this analysis is a Read-type structure with simulated doping profile N^+PIP^+ shown in Fig. 2. The electric field is approximated by a narrow high-field region in which both carrier generation and drift occur, and a lower field region having no ionization where carriers drift at saturated velocities. It is also assumed that the hole and electron ionization rates and drift velocities are equal, that is, $\alpha = \beta$, $v_n = v_p = v$.

For this structure, the sum of the hole and electron continuity equations integrated over the length of the avalanche zone ℓ_a yield the well-known Read equation [3] (neglecting saturation currents)

$$\frac{\ell_a}{v}\frac{d_{jC}}{dt} = 2j_C\left[\int_0^{\ell_a} \alpha\, dx - 1\right], \tag{4}$$

where $j_C(t)$ is the conduction current in the avalanche zone and is assumed to be independent of distance in this narrow zone. This assumption is equivalent to having no spacial variation of the total time-variant electric field in this zone. Therefore the field in the avalanche zone is

$$e_A(x, t) = E_A + e_a(t), \tag{5}$$

where E_A is the static field and e_a the ac component.

To derive the first-order nonlinear model, we use a first-order expansion of $\alpha(e_A)$ about E_A in (4) giving

$$\frac{1}{v}\frac{dj_C}{dt} = 2\alpha'(E_A)\, j_C e_a, \tag{6}$$

since E_A is the critical field and $\alpha(E_A)\,\ell_a = 1$. The field e_a is influenced both by the diode terminal voltage v_D and by the action of the charge (holes) in the drift zone in changing it through Poisson's equation. For this device of width W, the relationship has been determined by Evans [2] as

$$e_a(t) = \frac{v_D(t)}{W} - E_B - \frac{v}{\epsilon W}\int_{t-\tau}^{t} (\tau - t + t')\, j_C(t')\, dt', \tag{7}$$

where τ is the transit time of carriers through the drift zone and E_B is a constant equal to the effective dc electric field just at breakdown, that is, $E_B = V_B/W$.

If (7) is substituted in (6) an equation is obtained relating j_C in the avalanche zone to the terminal voltage v_D. This particle current is injected into the drift zone as holes and the total circuit current j_D at time t can be obtained by summing all the particle current injected from $t - \tau$ to t and adding the displacement current, giving

$$j_D(t) = \frac{\epsilon}{W}\frac{dv_D}{dt} + \frac{1}{\tau}\int_{t-\tau}^{t} j_C(t')\, dt'. \tag{8}$$

This equation may be regarded as the diode terminal relation because $j_C(t)$ can in principle be written in terms of v_D from (6) and (7).

To simplify this terminal relation, we assume that $j_C(t')$ is slowly variant over the interval $t' = t - \tau$ to $t' = t$, and may be expanded as

$$j_C(t') = j_C(t) + \left.\frac{dj_C}{dt'}\right|_t (t'-t). \tag{9}$$

This gives for e_a in (7)

$$e_a = \frac{v_D}{W} - E_B - \frac{\tau}{2\epsilon} j_C(t) + \frac{\tau^2}{6\epsilon}\frac{dj_C}{dt}. \tag{10}$$

Now using (10) in (6) results in a nonlinear differential equation for the conduction current j_C in terms of $v_D(t)$ as

$$\left(\frac{\tau}{2a'}\,\frac{1}{j_C} - \frac{W\tau^2}{6\epsilon}\right)\frac{dj_C}{dt} + \frac{\tau W}{2\epsilon}\,j_C(t) = v_D(t) - V_B. \tag{11}$$

This equation is similar to that derived by Evans [2]. We now change current density to total current by multiplying by the diode area A, and write (11) as

$$\left(\frac{\lambda_o}{i_C} - L_d\right)\frac{di_C}{dt} + Ri_C = v_D(t) - V_B, \tag{12}$$

where

$$\lambda_o = \frac{\tau}{2a'}\ \text{V-s} \tag{13a}$$

$$L_d = \frac{\tau^2 W}{6\epsilon A}\ \text{H} \tag{13b}$$

$$R = \frac{\tau W}{2\epsilon A}\ \Omega. \tag{13c}$$

Note that R is the space-charge resistance and is equal to $\tau/2C_d$, where C_d is the depletion layer capacitance $\epsilon A/W$.

To obtain the total diode current, (9) is used in (8) giving

$$i_D(t) = i_C(t) - \frac{\tau}{2}\frac{di_C}{dt} + C_d\frac{dv_D}{dt}. \tag{14}$$

It is now apparent that (14) and (12) can be modeled by the nonlinear equivalent circuit shown in Fig. 3. The series R-L branch is a model of (12), the controlled source represents the second current component of (14), and the capacitance represents the displacement component of (14). The terminal voltage of the model is taken as $v_D - V_B$, or the total voltage above the breakdown voltage.

The model has a restriction on the highest frequency allowable in the voltage or current waveforms because of the approximation given by (7). This restriction is equivalent to stating that the highest frequency f_{max} in the waveforms must be such that $f_{max}\tau \ll 1$.

IV. A PROPOSED FIRST-ORDER NONLINEAR CIRCUIT MODEL FOR EXISTING DIODES

By considering incremental sinusoidal voltage and current variations, the admittance of the circuit shown in Fig. 3 can be determined as

$$y_d' = \frac{1}{R' + j\omega L'} - G' + j\omega C_d, \tag{15}$$

where R', L', and G' are constant with respect to frequency but depend on bias current I_D as

$$G' = \frac{\tau/2}{\lambda_o/I_D - L_d} \tag{16a}$$

$$R' = \frac{R}{1 + RG'}. \tag{16b}$$

The quantities τ, λ_o, L_d, R and C_d were defined in Section III. For normal values of bias, $\lambda_o/I_D \gg L_d$ and $RG' \ll 1$, resulting in a simplification of (16) to

$$G' = \frac{\tau}{2\lambda_o} I_D \tag{17a}$$

$$L' = \frac{\lambda_o}{I_D} \tag{17b}$$

$$R' = R. \tag{17c}$$

It is apparent from the equations above that the small-signal elements for the model of Fig. 3 have nearly the same bias dependence as the elements in the small-signal model derived from measurements, shown in Fig. 1. This fact allows one to hypothesize that the basic topology of a possible nonlinear circuit model for an existing diode could be of the form shown in Fig. 3. In the following analysis it is assumed this is the case when developing the model.

The total diode current i_D is thus broken into three components: a current i_L in a branch containing a nonlinear inductance in series with a nonlinear resistance; a current i_G dependent (possibly nonlinearly) on the time-derivative of i_L; and a displacement current i_C in a shunt capacitance. Therefore if v_D is the total diode voltage (minus the breakdown voltage), then i_L, i_G, and i_C will be solutions of

$$L_1(i_L)\frac{di_L}{dt} + R_1(i_L)\, i_L = v_D(t), \tag{18a}$$

$$i_G = -\tau_1(i_L)\frac{di_L}{dt}, \tag{18b}$$

$$i_C = C_d\frac{dv_D}{dt}, \tag{18c}$$

and

$$i_D = i_L + i_G + i_C, \tag{18d}$$

where $L_1(i_L)$, $R_1(i_L)$, $\tau_1(i_L)$ and C_d are to be determined under the constraint that the small-signal diode admittance available from (18) has the observed bias (I_D) dependence. Note that the static bias current will exist entirely in the R-L branch, since the other two currents depend on time derivatives.

The functional form of $L_1(\cdot)$, $R_1(\cdot)$, and $\tau_1(\cdot)$ can be obtained by matching the small-signal characteristics available from (18) to those determined from measurements. It has been tacitly assumed that C_d is a constant and equal to the depletion capacitance. This assumption is valid if the space-charge width does not change appreciably with bias, as was the case for the measured diodes. Using incremental sinusoidal voltage and current variations, the admittance from (18) can be written as

$$y_1(j\omega) = \frac{1 + \tau_1(I_D)R_1(I_D)/L_1(I_D)}{R_1(I_D) + j\omega L_1(I_D)} - \frac{\tau_1(I_D)}{L_1(I_D)} + j\omega C_d. \tag{19}$$

Equating this admittance to that determined by measurement then requires

$$C_d = C_o \tag{20a}$$

$$\frac{\tau_1(I_D)}{L_1(I_D)} = G_o(I_D) \tag{20b}$$

$$\frac{R_1(I_D)}{1 + \tau_1(I_D)\, R_1(I_D)/L_1(I_D)} = R_o(I_D) \tag{20c}$$

$$\frac{L_1(I_D)}{1 + \tau_1(I_D)\, R_1(I_D)/L_1(I_D)} = L_o(I_D), \tag{20d}$$

where C_o, R_o, L_o, and G_o are the experimentally determined circuit elements obtained by data-reduction techniques. Inverting equations (20b)-(20d) shows that

$$\tau_1(I_D) = L_o(I_D)\, G_o(I_D), \tag{21a}$$

$$R_1(I_D) = \frac{R_o(I_D)}{1 - R_o(I_D)\, G_o(I_D)}, \tag{21b}$$

$$L_1(I_D) = \frac{L_o(I_D)}{1 - R_o(I_D)\, G_o(I_D)}. \tag{21c}$$

These equations determine the functional form of the elements in the proposed nonlinear circuit model. For values of bias where the empirically determined model is valid, the factor $R_o G_o$ is normally small compared to unity and can be neglected in equations (21b) and (21c). Then using the typical bias variations given in Fig. 1, (21a)-(21c) reduce to

$$\tau_1 = L_o G_o = \lambda\gamma = \text{const}, \tag{22a}$$

$$R_1 = R_o, \tag{22b}$$

$$L_1(I_D) = \frac{\lambda}{I_D}. \tag{22c}$$

The nonlinear model for elements with these characteristics is shown in Fig. 4. If the small-signal model elements do not have the simple form used in obtaining (22), then (21) must be used to determine the functional form of the elements in the nonlinear model. The main difference between the two models is that in the experimental characterization $\tau_1 \neq 2RC_d$. It should be expected that this model, like that of Fig. 4, is limited to frequencies f such that $f\tau_1 \ll 1$. Since τ_1 is normally of the order of 20 ps for X-band devices, analysis should be limited to below ~10 GHz.

A semiempirical nonlinear circuit model for the avalanche diode has been proposed by working from measured small-signal impedance data, assuming the form of the model would be similar to that for an idealized diode. Because of the assumed similarity the elements relate to the physical electronics of the diode, and in this sense the model is appealing. In most cases the values of the constants R_o, τ_1, and λ could be determined by the simplified measurement technique described elsewhere [1].

The model was developed as a means for describing the diode terminal behavior in response to intermediate-amplitude or multiple-frequency (two-tone) signals. If the model can be proved in this sense then it would be useful in establishing some performance limitations on avalanche diode circuits caused by nonlinear effects. In Section V, the model is shown to be capable of predicting intermodulation distortion and gain compression in avalanche diode amplifiers.

V. PREDICTIONS OF INTERMODULATION DISTORTION AND GAIN COMPRESSION IN AVALANCHE DIODE AMPLIFIERS

In this section, expressions are developed for the intermodulation distortion and gain compression in avalanche diode amplifiers and the results are compared with experiment. The results are seen to be in close agreement.

The analysis will use the normalized wave variables, since their magnitudes squared determine power levels which are easily measured at microwave frequencies. First we discuss intermodulation distortion.

Consider the circuit of Fig. 5 in which the circulator (not shown) is assumed to be connected to terminals 1-1' so that the input wave is $a_1(t)$ and the output wave is $b_1(t)$. The frequencies of the input wave are constrained by the source to be ω_1 and ω_2, where $|\omega_2-\omega_1| = \Delta\omega$. The input-wave amplitude at each of these frequencies will be denoted by A_{11}, so that the power carried in each wave at the input is $|A_{11}|^2$. The amplitudes of the frequencies existing in the output wave $b_1(t)$ must now be determined.

Since the diode is defined in terms of voltage and current, we must first relate these to the wave variables at port 2 of the coupling network. Then, by using the scattering parameters to interrelate the wave variables at ports 1 and 2, the output wave b_1 is determined in terms of a_1 and network parameters.

At port 2 of the network, the normalized wave variables can be defined in terms of the voltage and current as

$$A_2(\omega) = \frac{-I_2(\omega) + Y_c(\omega)\, V_2(\omega)}{2\sqrt{2G_c(\omega)}} \tag{23a}$$

$$B_2(\omega) = \frac{-I_2(\omega) - Y_c^*(\omega)\, V_2(\omega)}{2\sqrt{2G_c(\omega)}}, \tag{23b}$$

where V_2 and I_2 will be the diode voltage and current peak amplitudes at any frequency ω. Also, from the scattering parameters of the coupling network,

$$B_1(\omega) = s_{11}(\omega)\, A_1(\omega) + s_{12}(\omega)\, A_2(\omega) \tag{24a}$$

$$B_2(\omega) = s_{21}(\omega)\, A_1(\omega) + s_{22}(\omega)\, A_2(\omega). \tag{24b}$$

By specifying the normalization admittance $Y_c(\omega)$ at port 2 of the coupling network the analysis is considerably simplified. Because the network is assumed lossless, the scattering parameters obey the relations

$$|s_{11}| = |s_{22}| \tag{25a}$$

$$|s_{12}|^2 = |s_{21}|^2 = 1 - |s_{22}|^2, \tag{25b}$$

and therefore if we can choose Y_c so that $|s_{11}| = 0$, the relations in (24) will be simplified considerably. From (24b)

$$s_{22} = \left.\frac{B_2}{A_2}\right|_{A_1=0}. \tag{26}$$

Since port 1 is always terminated in its reference impedance when the circulator is connected, s_{22} can be made zero by choosing Y_c as the complex conjugate of the impedance observed by looking into port 2 because then

$$B_2 = \frac{\left(-I_2/V_2 - Y_c^*\right)V_2}{2\sqrt{2G_c}} = \frac{\left(Y_c^* - Y_c^*\right)V_2}{2\sqrt{2G_c}} = 0.$$

Thus $|s_{11}|$ is also equal to zero and $|s_{12}| = 1$, so the scattering relations (24) reduce to

$$B_1(\omega) = s_{12}(\omega)\,A_2(\omega) \tag{27a}$$

$$B_2(\omega) = s_{21}(\omega)\,A_1(\omega). \tag{27b}$$

These equations are strictly valid only at one frequency; if the frequency is changed, Y_c must also be changed. In this analysis, we will be concerned with a narrow band of frequencies centered around $(\omega_1+\omega_2)/2 = \omega_o$, within which it is assumed that Y_c remains essentially constant. This puts the following restriction on the frequency difference $\Delta\omega$ of the two-tone.

RESTRICTION: In order that the calculated n^{th} odd-order distortion products of an avalanche diode amplifier be compatible with their experimental measurement, the frequency difference $\Delta\omega = |\omega_1 - \omega_2|$ of the two-tone must be such that

$$n\Delta\omega \ll \frac{\omega_1 + \omega_2}{2}, \quad n \text{ odd}. \tag{28}$$

This is equivalent to stating that the bandwidth of the amplifier is large compared with the band of frequencies containing the n^{th} odd-order distortion terms.

This restriction also allows one to state that if the input is an equal-amplitude two-tone, the amplitudes of the corresponding n^{th} odd-order distortion products in each sideband at the output will be nearly equal, and only a single sideband need be analyzed.

The relations given in (27) are therefore assumed valid for all frequencies in the narrow band which was considered. The wave b_2 has the same frequency components as a_1 (only at ω_1 and ω_2) and the wave a_2 will contain frequency components at the intermodulation products which are observed in the output. In both cases the amplitudes will be equal, since $|s_{12}|$ and $|s_{21}|$ are equal to unity.

In a single sideband, b_2 has only one frequency component, B_{21}, at one of the two input frequencies, whereas a_2 will have components at the odd-order distortion frequencies which are denoted by A_{2n}, $n = 1, 3, 5 \ldots$. From (23), the diode voltage and current will similarly contain components at all the distortion product frequencies. Denote these components by V_{dn} and I_{dn}, $n = 1, 3, 5 \ldots$, then (23b) implies

$$\frac{-Y_c^* V_{d1} - I_{d1}}{2\sqrt{2G_c}} = B_{21} = \frac{A_{11}}{s_{21}} \tag{29a}$$

and

$$\frac{-Y_c^* V_{dn} - I_{dn}}{2\sqrt{2G_c}} = 0. \tag{29b}$$

It is shown in the Appendix that when the diode just begins to deviate from linearity, the odd-order nonlinearities of the diode give the following relations between V_{dn} and I_{dn}:

$$V_{d1} = Z_d I_{d1} \tag{30a}$$

$$V_{dn} = Z_d I_{dn} + K_{1n} I_{d1}^n \qquad n = 3, 5, 7, \tag{30b}$$

where V_{dn} and I_{dn} are peak amplitudes and satisfy the constraints $|V_{dn}|/|V_{d1}| \ll 1$ and $|I_{dn}|/|I_{d1}| \ll 1$, $n = 3, 5, 7, \ldots$. Thus from (29a)

$$\frac{A_{11}}{s_{21}} = \frac{I_{d1}\left(1+Y_c^* Z_d\right)}{2\sqrt{2G_c}}$$

or

$$I_{d1} = \frac{2\sqrt{2G_c}\, s_{21}}{1 + Y_c^* Z_d} A_{11}, \tag{31a}$$

and from (29b)

$$I_{dn} = -\frac{Y_c^* K_{1n} I_{d1}^n}{1 + Y_c^* Z_d}. \tag{31b}$$

Equation (31a) gives the amplitude of the diode current at the two-tone frequency in terms of the input-wave amplitude A_{11}, and (31b) is a constraint on the amplitudes of the diode distortion currents, given I_{d1}. The amplitudes of the terms in the output wave b_1 can be determined by using (23a).

$$A_{21} = \frac{B_{11}}{s_{12}} = \frac{-I_{d1}(1-Y_c Z_d)}{2\sqrt{2G_c}} \tag{32a}$$

$$A_{2n} = \frac{B_{1n}}{s_{12}} = \sqrt{\frac{G_c}{2}}\,\frac{K_{1n} I_{d1}^{n}}{1 + Y_c^{*} Z_d} \,. \tag{32b}$$

By combining (31a) with (32) the output-wave amplitudes can be obtained in terms of the input wave A_{11} as

$$B_{11} = -s_{12}s_{21}\,\frac{1 - Y_c Z_d}{1 + Y_c^{*} Z_d}\,A_{11} = \Gamma A_{11} \tag{33a}$$

$$B_{1n} = s_{12}s_{21}^{n}(2)^{(3n-1)/2}\,\frac{(G_c)^{(n+1)/2}\,K_{1n}}{\left(1+Y_c^{*}Z_d\right)^{n}}\,A_{11}^{n} \qquad n = 3, 5, \ldots . \tag{33b}$$

Note that (33a) is just the small-signal gain equation. The n^{th} odd-order intercept referred to the input is that value of input power $|A_{11}|^2$ such that at the output $|B_{1n}| = |B_{11}|$ if B_{11} and B_{1n} were to continue to vary with A_{11} as in (33). Therefore,

$$I_n = \frac{1}{4}\left[\frac{|\Gamma|\,|1+Y_c^{*}Z_d|^{n+1}}{(2G_c)^{(n+1)/2}\,|K_{1n}|}\right]^{2/(n-1)} \qquad n = 3, 5, 7, \ldots . \tag{34}$$

As stated earlier, the normalizing admittance Y_c is the conjugate of the admittance Y_L seen by looking into port 2 of the coupling network. Since the amplifier is to have gain, Y_L will be carefully designed in the passband of the amplifier in relation to Z_d. From (33a)

$$\rho = |\Gamma| = \left|\frac{Y_d - Y_L^{*}}{Y_d + Y_L}\right| = \left|\frac{-G_d - G_L + j(B_d + B_L)}{-G_d + G_L + j(B_d + B_L)}\right|, \tag{35}$$

and if the amplifier is tuned so that $B_L = -B_d$,

$$\rho = \left| \frac{G_L + G_d}{G_L - G_d} \right|, \tag{36}$$

and (34) can be written as

$$I_n = \frac{1}{4}\left[\rho \left(\frac{2G_d |Z_d|^2}{\rho^2 - 1} \right)^{(n+1)/2} \cdot \frac{1}{|K_{1n}|} \right]^{2/(n-1)} . \tag{37}$$

In the Appendix it is shown that for the avalanche diode nonlinear model, $|K_{1n}|$ is given by

$$|K_{1n}| = \frac{\omega L |Z_d|^{n+1} a_n \alpha}{I_o^{n-1} |R + j\omega L + r_s \beta|^{n+1}}, \tag{38}$$

where α, R, L, β and r_s are small-signal diode parameters, I_o is bias current, and a_n is given [4] by

$$a_n = \frac{(n-1)!}{2^{n-1}\left(\frac{n+1}{2}\right)! \cdot \left(\frac{n-1}{2}\right)!} \qquad n = 3, 5, 7. \tag{39}$$

By substituting $|K_{1n}|$ in (37), the final expression for the odd-order intercept is

$$I_n = \frac{I_o^2}{4}\left[\frac{2G_d |R + j\omega L + \beta r_s|^2}{\rho^2 - 1} \right]^{(n+1)/(n-1)} \left[\frac{\rho}{\omega L a_n \alpha} \right]^{2/(n-1)} . \tag{40}$$

For most diodes, $R + \mathrm{Re}\{\beta r_s\} \ll \omega L + \mathrm{Im}\{\beta r_s\}$ and $\mathrm{Im}\{\beta r_s\} \ll \omega L$. Therefore (40) can be simplified slightly to become

$$I_n = \frac{I_o^2}{4}\left[\frac{2G_d}{\rho^2 - 1} \right]^{(n+1)/(n-1)} \left[\frac{\rho}{\alpha a_n} \right]^{2/(n-1)} (\omega L)^{2n/(n-1)} . \tag{41}$$

In the derivation of (40) several other mixing processes which can occur in the diode and influence the amount of intermodulation distortion have been neglected. These effects include mixing between intermod products themselves and down conversion from higher harmonics. These effects are negligible at low input power and their eventual influence on the intermods serves to define the limits of the well-behaved region of operation.

Gain compression is determined by driving the amplifier with a single tone and finding the amount of gain reduction as the input signal power is increased. As in the previous case, neither the diode voltage nor diode current can be constrained to be a single frequency; each will contain harmonics of the frequency of the applied signal. Since we are primarily interested in the region of operation where the gain just begins to deviate from its small signal-value, an assumption can be made about the harmonic content of the diode voltage and current waveforms. The assumption is that the ac component of diode current in the R-L branch of the nonlinear model consists primarily of a fundamental component. This assumption is discussed further in the Appendix.

Therefore $i_L(t)$ can be written as

$$i_L(t) \approx I_L + I_\ell \cos \omega_o t, \tag{42}$$

where $I_\ell < I_L$ and I_L is the diode bias current. By using this form for the current, the total diode voltage and current at frequency ω_o are shown in the Appendix to be

$$I_d = \beta I_\ell - \omega_o^2 LCrI_\ell \tag{43}$$

$$V_d = (R+j\omega_o L+\beta r_s)I_\ell + \left(j\omega_o L-\omega_o^2 LCr_s\right)rI_\ell, \tag{44}$$

where r is a function of (I_ℓ/I_L) as

$$r = \frac{1 - \sqrt{1 - (I_\ell/I_L)^2}}{1 + \sqrt{1 - (I_\ell/I_L)^2}}. \tag{45}$$

Using these equations, one can determine the amplitudes of the input and output waves $|A_{11}|$ and $|B_{11}|$ from (23a) and (23b), thereby obtaining the gain ρ in terms of I_ℓ. The relation can be inverted to give I_ℓ in terms of the gain ρ, which can then be substituted in the equation for $|A_{11}(I_\ell)|$ (see Appendix) to yield $|A_{11}(\rho)|$, where

$$P_{in}(\rho) = |A_{11}(\rho)|^2 = \frac{4|R+j\omega_o L+\beta r_s|^2 I_L^2 G_d}{(\rho_o-1)^2(\rho+1)^2}(\rho_o-\rho). \tag{46}$$

In this expression, ρ_o is the small-signal gain, ρ is the gain at arbitrary input power and is subject to the constraint

$$\rho_o \geq \rho \geq \frac{3\rho_o + 1}{\rho_o + 3} \tag{47}$$

in order that I_ℓ remain less than I_L. Equation (46) gives the input power in terms of the gain, which is the inverse of the usually desired relation. In order to obtain $\rho(P_{in})$, however, a quadratic equation must be solved and the result is more difficult to interpret than (47). For instance, (47) allows one to easily obtain the standard 1-dB gain compression point by letting $\rho = 0.891\rho_o$ as

$$P_{-1\,dB} \cong \frac{.436(\omega L)^2 I_L^2 G_d \rho_o}{(\rho_o-1)^2(.891\rho_o+1)^2}, \tag{48}$$

where the same approximations were used as in obtaining (41).

Combining (48) and (41) for n = 3, the third-order intercept can be related to the 1-dB compression point as

$$\frac{I_3}{P_{-1\,dB}} = 7.28\left(\frac{\omega_o L G_d}{a}\right)\cdot\left(\frac{\rho_o+1.122}{\rho_o+1}\right)^2 \tag{49a}$$

$$\approx 7.28\left(\frac{\omega_o L G_d}{a}\right), \qquad \rho_o \gg 1 \tag{49b}$$

and only one of these quantities need be calculated or measured to determine the other.

VI. MEASUREMENT OF AMPLIFIER INTERCEPTS AND GAIN COMPRESSION, AND COMPARISON WITH THEORY

In order that a measurement of the intermodulation distortion in an amplifier be compatible with the theory, the experiment must conform to the constraints and assumptions discussed previously. The test arrangement for the measurement of intermodulation distortion is shown in Fig. 6. Signals at frequencies f_1 and f_2 are fed through attenuators and isolators into a hybrid which for this case was a waveguide magic tee. The sum of the signals went into a 3-port circulator attached to the amplifier. The amplified signals were then attenuated and fed into a double balanced mixer having a phase-locked source as local oscillator. The down-converted signals could then be observed in a conventional low-frequency spectrum analyzer. The reason for the down-conversion by way of the mixer was to improve resolution of the signals, since the frequency difference of the two-tone was kept at less than 2 mHz. Attenuation in front of the mixer was used to keep power level entering the mixer low enough to prevent any appreciable intermod generation within the mixer itself. The dynamic range of the mixer-spectrum analyzer combination was much better than that of the amplifier. The input power level to the amplifier was obtained by replacing the amplifier with a matched power meter and calibrating one of the input attenuators so that the power level in the input wave to the amplifier was known from the attenuator setting.

The output on the spectrum analyzer was calibrated by setting the input power to a low value (~-30 dBm) where no gain compression occurred and adjusting the spectrum analyzer display reference to read the correct value of output power (input power in dBm + gain of amplifier in dB). Then as the amplitude of the two-tone was increased, the absolute power levels in the distortion products were read directly from the analyzer.

The gain compression and passband characteristics of the amplifiers were measured using only one signal.

Measured Amplifier Intercepts and Gain Compression and Correlation with Theory

Measurements were made on three separate amplifiers each having a diode which had known small-signal circuit parameters λ_o, R, G, C, and r_s, determined from de-embedded measurements. Two of these diodes, the Varian and the Sylvania were silicon diffused P^+NN^+ types and the third was a double-diffused $P^+N^-NN^+$ T.I. Read-type structure. The results of the measurements and the calculated results for each of these amplifiers using the equation derived in Section III are shown in Table 1. The actual measured data taken on each of the amplifiers are shown in Figs. 8, 9, 10. Figure 7 shows the calculated curves for amplifier 1. In each case the odd-order distortion product curves appeared to have the correct slopes at low input power levels. These slopes should be 3, 5, 7, etc. on the P_{out} versus P_{in} graph. The largest amount of data was available in each case for the third-order products, while for the seventh-order terms, little or no data were available in the well-behaved region where these products should be increasing seven times as fast as P_i. This means that one should not weigh the seventh-order data very heavily as a measure of the validity of the model.

VII. CONCLUSION

The main conclusion to be drawn from this study is that the proposed nonlinear circuit model is capable of predicting some of the performance degradations observed in avalanche diode amplifiers. This result gives partial proof that the model may reliably describe the diode terminal behavior for other than small signals, and therefore might be useful in determining and predicting performance of other circuits which use the diode in a nonlinear manner, such as frequency converters or self-pumped parametric amplifiers. Since the constants in the model can usually be obtained in a straightforward manner by using the characterization technique presented in [1], the problem of matching a diode to a circuit for a desired performance is partially overcome by prior knowledge of the device terminal behavior.

APPENDIX

DERIVATION OF EQUATIONS FOR PREDICTING INTERMODULATION AND GAIN COMPRESSION IN AVALANCHE DIODE AMPLIFIERS USING THE PROPOSED NONLINEAR CIRCUIT MODEL

For the reflection amplifier, the input-wave variable is constrained to be a two-tone, so that at the terminals of the nonlinear device (the diode) neither the diode voltage nor current will be strictly a two-tone. Each will contain intermodulation distortion terms and these must be considered in carrying out the analysis.

With this consideration, the current in the nonlinear R-L branch of the equivalent circuit model will be specified as

$$i_L(t) = I_L + i_\ell(t) + \delta i_\ell(t), \tag{A-1}$$

where

$$i_\ell(t) = I_{\ell 1}(\cos \omega_1 t + \cos \omega_2 t), \tag{A-2}$$

and $\delta i_\ell(t)$ is a perturbation current that has components at the distortion-product frequencies. It has been assumed in (A-2) that the currents in each sideband will have approximately equal amplitudes at corresponding frequencies, a valid assumption in this case if $|\omega_1 - \omega_2| \ll \omega_1$ or ω_2. This assumption is also made for corresponding complex amplitudes in $\delta i_\ell(t)$; that is, the component at $(2\omega_1 - \omega_2)$ is equal to the one at $(2\omega_2 - \omega_1)$, and so forth.

Using (A-1), the voltage v_L across the nonlinear inductance can be determined, and in particular the odd-order distortion voltages can be obtained in a simple manner by writing

$$v_L = \frac{\lambda_o}{i_L}\frac{di_L}{dt} = \lambda \frac{d}{dt} \ell n\, i_L = \lambda_o \frac{d}{dt} \ell n \left(1 + \frac{i_\ell + \delta L_\ell}{I_L}\right), \tag{A-3}$$

which can be expanded at low levels when $|i_\ell+\delta i_\ell|/I_L < 1$ as

$$v_L = \lambda_o \frac{d}{dt} \sum_{n=1}^{\infty} \frac{(-1)^{n-1}}{n} \left(\frac{i_\ell+\delta i_\ell}{I_L}\right)^n . \tag{A-4}$$

The odd-order distortion terms will come from the odd-order nonlinearities in the summation. A restriction is now made which is necessary for operation in the well-behaved region of the amplifier. Since δi_L is a perturbation current, it is assumed that the amplitudes of its currents are small compared with $I_{\ell 1}$ and it is retained only in the linear term of the expansion. At the frequencies around the two-tone, the components of $\delta i_\ell(t)$ in one sideband will be written as $\delta i_{\ell s}(t)$, where

$$\delta i_{\ell s}(t) = \mathrm{Re}\left\{ I_{\ell 3} e^{j(2\omega_1-\omega_2)t} + I_{\ell 5} e^{j(3\omega_1-2\omega_2)t} + \ldots \right\}, \tag{A-5}$$

where the $I_{\ell n}$'s may be complex. The other sideband will contain equal amplitude components. If (A-2) is now substituted in (A-4) and the distortion terms are collected at the various frequencies, the complex amplitudes of the distortion components of v_L in a single sideband are then

$$v_{\ell 1} = j\omega_o\lambda_o\left[\frac{I_{\ell 1}}{I_L} + \frac{3}{4}\left(\frac{I_{\ell 1}}{I_L}\right)^3 + \frac{5}{4}\left(\frac{I_{\ell 1}}{I_L}\right)^5 + \ldots\right] \tag{A-6a}$$

$$v_{\ell 3} = j\omega_o\lambda_o\left[\frac{I_{\ell 3}}{I_L} + \frac{1}{4}\left(\frac{I_{\ell 1}}{I_L}\right)^3 + \frac{5}{8}\left(\frac{I_{\ell 1}}{I_L}\right)^5 \ldots\right] \tag{A-6b}$$

$$v_{\ell 5} = j\omega_o\lambda_o\left[\frac{I_{\ell 5}}{I_L} + \frac{1}{8}\left(\frac{I_{\ell 1}}{I_L}\right)^5 + \ldots\right] \tag{A-6c}$$

and so on, where $V_{\ell n}$ is the odd-order distortion voltage at $\frac{n+1}{2}\omega_1 - \frac{n-1}{2}\omega_2$, $n = 1, 3, 5 \ldots$ and ω_o has replaced ω_1, $2\omega_1 - \omega_2$, $3\omega_1 - 2\omega_2$, etc., since $|\omega_1-\omega_2| \ll \omega_1, \omega_2$.

If operation is restricted to the well-behaved region, $(I_{\ell 1}/I_L)^2 \ll 1$ and in general the n^{th} odd-order distortion voltage is written as

$$V_{\ell n} = j\omega_o\lambda_o\left[\frac{I_{\ell n}}{I_L} + a_n\left(\frac{I_{\ell 1}}{I_L}\right)^n\right] \qquad n = 3, 5, 7 \ldots, \tag{A-7}$$

where a_n can easily be determined by Steinbrecher's [4] algorithm as

$$a_n = \frac{(n-1)!}{2^{n-1}\left(\frac{n+1}{2}\right)! \cdot \left(\frac{n-1}{2}\right)!} \qquad n = 3, 5, 7. \tag{A-8}$$

Add the voltage across R caused by i_L to v_L, then the complex amplitudes of the distortion voltages V_n across the total diode equivalent circuit are

$$V_1 = RI_{\ell 1} + j\frac{\omega\lambda_o}{I_L} I_{\ell 1} \tag{A-9a}$$

$$V_n = RI_{\ell n} + j\frac{\omega\lambda_o}{I_L} I_{\ell n} + j\omega\lambda_o a_n\left(\frac{I_{\ell 1}}{I_L}\right)^n. \tag{A-9b}$$

The total diode complex current amplitudes are next determined by adding the currents in the other two branches of the equivalent circuit, that is, $-\tau\frac{di_L}{dt}$ and $C\frac{dv}{dt}$. This gives for the amplitudes of the diode currents at the distortion frequencies

$$I_{d1} = I_{\ell 1} - j\omega\tau I_{\ell 1} + j\omega C\left(R + j\frac{\omega\lambda_o}{I_L}\right) I_{\ell 1} \tag{A-10a}$$

$$I_{dn} = \left[1 - j\omega\tau + j\omega C\left(R + j\frac{\omega\lambda_o}{I_L}\right)\right] \cdot I_{\ell n} + j\omega C\left(j\frac{\omega\lambda_o}{I_L} a_n\right) \cdot \left(\frac{I_{\ell 1}}{I_L}\right)^n \tag{A-10b}$$

in terms of the current in the R-L branch. Since we consider in the amplifier analysis that r_s is part of the "diode," the total diode voltage

must include the drop across r_s caused by the total diode current (A-10). Thus for the total diode complex voltage amplitudes at the intermod frequencies, we have

$$V_{d1} = r_s I_{d1} + V_1 \tag{A-11a}$$

$$V_{dn} = r_s I_{dn} + V_n. \tag{A-11b}$$

From (A-10a) we can write that $I_{\ell 1} = I_{d1}/\beta$, where

$$\beta = 1 - j\omega\tau + j\omega C(R+j\omega L) \tag{A-12}$$

and $L = \lambda_o/I_L$. Then (A-9) can be written as

$$V_1 = \frac{R + j\omega L}{\beta} I_{d1} \tag{A-13a}$$

$$V_n = \frac{R + j\omega L}{\beta} I_{dn} + \frac{j\omega\lambda_o a_n}{\beta^{n+1}} (1-j\omega\tau)\left(\frac{I_{d1}}{I_L}\right)^n. \tag{A-13b}$$

These equations are substituted in (A-11) to give

$$V_{d1} = Z_d I_{d1} \tag{A-14a}$$

$$V_{dn} = Z_d I_{dn} + K_{1n} I_{d1}^n, \tag{A-14b}$$

where Z_d is the total diode impedance

$$Z_d = r_s + \frac{R + j\omega L}{\beta} \tag{A-15}$$

and K_{1n} is given by

$$K_{1n} = \frac{j\omega\lambda_o a_n (1-j\omega\tau)}{\beta^{n+1} I_L^n}. \tag{A-16}$$

Equation (A-14) was presented in Section V. Using these relations and the constraint equations developed in the text, the currents I_{d1} and I_{dn} can be determined in terms of the wave variables and the amplifier intercepts may then be obtained.

The gain compression in an amplifier is determined by assuming the current in the nonlinear inductor to be primarily at a single frequency, that of the input wave. This assumption is probably valid at least to the amplifier 1 dB compression point, beyond which harmonic mixing may influence the amplifier gain.

Since the time origin can be specified, we have for the inductor current $i_L(t)$

$$i_L(t) = I_L + I_\ell \cos \omega_o t \tag{A-17}$$

and thus

$$v_L(t) = \frac{-\omega_o \lambda_o I_\ell \sin \omega_o t}{I_L + I_\ell \cos \omega_o t}. \tag{A-18}$$

The component of this voltage at ω_o will be of sine phase, since v_L is odd and is given by

$$V_1 = \frac{-\omega_o \lambda_o I_\ell}{\pi I_L} \int_0^{2\pi} \frac{\sin^2 (\omega t)\, d(\omega t)}{1 + a \cos \omega t}. \tag{A-19}$$

This integral is tabulated [5] and yields

$$V_1 = \frac{-2\omega\lambda_o a}{1 + \sqrt{1 - a^2}}, \tag{A-20}$$

where $a = I_\ell / I_L < 1$. Add the voltage drop across the series resistor, then the voltage across the equivalent circuit v_e at ω_o is

$$v_e(t) = V_1 \sin \omega_o t + RI_\ell \cos \omega_o t$$

$$= \mathrm{Re}\left[(R + j\omega_o Lk) I_\ell e^{j\omega_o t}\right], \tag{A-21}$$

where $k = 2/(1+\sqrt{1-a^2})$. The total diode current is obtained by adding the other two components in the current source and capacitance as

$$I_d = \beta I_\ell - \omega^2 LCrI_\ell, \tag{A-22}$$

where

$$r = \frac{1-\sqrt{1-a^2}}{1+\sqrt{1-a^2}}. \tag{A-23}$$

Add the voltage drop across r_s to v_e, then the diode voltage amplitude is

$$V_d = Z_d \beta I_\ell + j\omega_o L(1+j\omega_o C r_s)\, rI_\ell \tag{A-24}$$

in terms of the current I_ℓ.

By using the equations for the wave amplitudes in terms of V_d and I_d developed in Section V, the magnitude of the reflection coefficient $\Gamma = B_{11}/A_{11}$ is given by

$$\rho = |\Gamma| = \left| \frac{G_c - G_d + r\gamma_1}{G_c + G_d + r\gamma_2} \right|, \tag{A-25}$$

where γ_1 and γ_2 are complex and are

$$\gamma_1 = \frac{j\omega L}{R + j\omega L + \beta r_s} \left[Y_c(1+j\omega r_s C) - j\omega C \right] \tag{A-26a}$$

$$\gamma_2 = \frac{j\omega L}{R + j\omega L + \beta r_s} \left[Y_c^*(1+j\omega r_s C) + j\omega C \right]. \tag{A-26b}$$

Note that as $I_\ell \to 0$, $r \to 0$ and ρ approaches its small-signal value, where

$$\rho_o = \frac{G_c - G_d}{G_c + G_d}. \tag{A-27}$$

For most avalanche diodes γ_1 and γ_2 can be simplified, since $\omega L \gg R$, $|\beta r_s| \ll \omega L$, $\omega r_s C \ll 1$, and $\omega C \approx B_d$, the susceptance of the diode. Then since the amplifier is "tuned," $\mathrm{Im}\{Y_c\} = B_d$ and (A-25) reduces to

$$\rho = \frac{G_c - G_d + rG_c}{G_c + G_d + rG_c}, \tag{A-28}$$

or, in terms of the small-signal gain ρ_o,

$$\rho = \frac{\rho_o + \frac{r}{2}(\rho_o+1)}{1 + \frac{r}{2}(\rho_o+1)}. \tag{A-29}$$

Equation (A-29) can be solved for r from which $(I_\ell/I_L)^2$ can be determined as

$$\left(\frac{I_\ell}{I_L}\right)^2 = 1 - \left[\frac{2(\rho_o+1)(\rho-1)}{(\rho_o-1)(\rho+1)} - 1\right]. \tag{A-30}$$

Therefore I_ℓ is determined in terms of the gain of the amplifier at any value of input level. Once we have obtained I_ℓ, the magnitude of the input wave $|a_{11}|^2$ which depends on I_ℓ can be written in terms of ρ and ρ_o. In terms of I_ℓ, by using the expressions for V_d and I_d (A-22) and (A-24) and simplifying, $|a_{11}|$ is given by

$$|a_{11}| = \frac{|R+j\omega L+\beta r_s|\, G_d I_\ell}{\sqrt{2G_c}\,(\rho_o-1)} \left[1 + \frac{\rho_o+1}{2}\, r\right] \tag{A-31}$$

which after using (A-30), squaring, and simplifying, results in

$$P_{in}(\rho) = |a_{11}|^2 = \frac{4|R+j\omega L+\beta r_s|^2 G_d I_L^2(\rho_o-\rho)}{(\rho_o-1)^2(\rho+1)^2}. \qquad \text{(A-32)}$$

This result was presented as Eq. (46). Since I_ℓ/I_L must be less than unity, (A-32) is mathematically valid only for values of ρ such that

$$\rho_o > \rho > \frac{3\rho_o + 1}{3 + \rho_o} \qquad \text{(A-33)}$$

determined from (A-29).

TABLE I

Comparison of Computed and Measured Intermodulation Distortion and Gain Compression for Avalanche Diode Amplifiers

Data \ Amplifier	1	2	3
Diode	Varian 9DH-1-9	Sylvania	Texas Instrument Read-I-4H
Bias-I_o	23 mA	38 mA	22 mA
$L = \lambda_o/I_o$	4.53 nH	4.0 nH	4.04 nH
C pF	.75	.44 pF	.45 pF
G mhos	.0015	.0028	.0027
R Ω	14.6	11.0	33.7
r_s Ω	.58	1.3	.43
Gain dB	13.6	17.6	18.5
Bandwidth (mHz)	125	75	100
fo (Gc)	9.67	9.9	9.125
1 dB MGCP*	-6.8 dBm	-5.4 dBm	-9.5 dBm
1 dB CGCP†	-7.1 dBm	-7.14 dBm	-11.6 dBm
I_3 (meas)	-2.5 dBm	-3.6 dBm	-7.5 dBm
I_3 (calc)	-3.46 dBm	-3.0 dBm	-8.3 dBm
I_5 (meas)	-1.5 dBm	-3.0 dBm	-6.1 dBm
I_5 (calc)	-.47 dBm	+.05 dBm	-4.7 dBm
I_7 (meas)	-.75 dBm	-	-3.6 dBm
I_7 (calc)	.017 dBm	+1.57 dBm	-3.32 dBm
Figures	11	12	13

*Measured Gain Compression Point.

†Calculated Gain Compression Point.

Footnotes

Manuscript received . The work was supported in part by the National Aeronautics and Space Administration (Grant NGL 22-009-337) and in part by the Joint Services Electronics Program (Contract DAAB07-71-C-0300).

D. H. Steinbrecher is with the Department of Electrical Engineering and the Research Laboratory of Electronics, Massachusetts Institute of Technology, Cambridge, Mass. 02139.

D. F. Peterson is now with M. I. T. Lincoln Laboratory, Lexington, Mass. 01773.

References

[1] D. H. Steinbrecher and D. F. Peterson, "Small-signal model with frequency-independent elements for the avalanche region of a microwave negative-resistance diode," IEEE Trans. on Electron Devices, vol. ED-17, no. 10, pp. 883-891, October 1970.

[2] W. J. Evans, "Nonlinear and frequency conversion characteristics of IMPATT diodes," Technical Report 104, Electron Physics Laboratory, University of Michigan, Ann Arbor, Mich., February 1968.

[3] W. T. Read, "A proposed high-frequency, negative resistance diode," Bell Syst. Tech. J., vol. 33, pp. 401-446, March 1954.

[4] D. H. Steinbrecher, "An Algorithm for Computing Intermodulation Distortion Product Amplifiers" (unpublished).

[5] P. Penfield, Jr., "Fourier coefficients of power-law devices," J. Franklin Inst., vol. 273, no. 2, p. 109, February 1962.

FIGURE CAPTIONS

Fig. 1. First-order model of measured admittance.

Fig. 2. Idealized two-zone avalanche diode structure.

Fig. 3. Equivalent circuit model of idealized two-zone diode for large signals.

Fig. 4. First-order nonlinear circuit model proposed for existing diodes.

Fig. 5. Amplifier network used in the analysis of intermodulation distortion and gain compression.

Fig. 6. Experimental setup for measurement of intermodulation distortion and gain compression in avalanche diode amplifiers.

Fig. 7. Theoretical intercepts and gain compression for amplifier 1.

Fig. 8. Measured IMD and gain compression characteristics for amplifier 1.

Fig. 9. Measured IMD and gain compression for amplifier 2.

Fig. 10. Measured IMD and gain compression for amplifier 3.

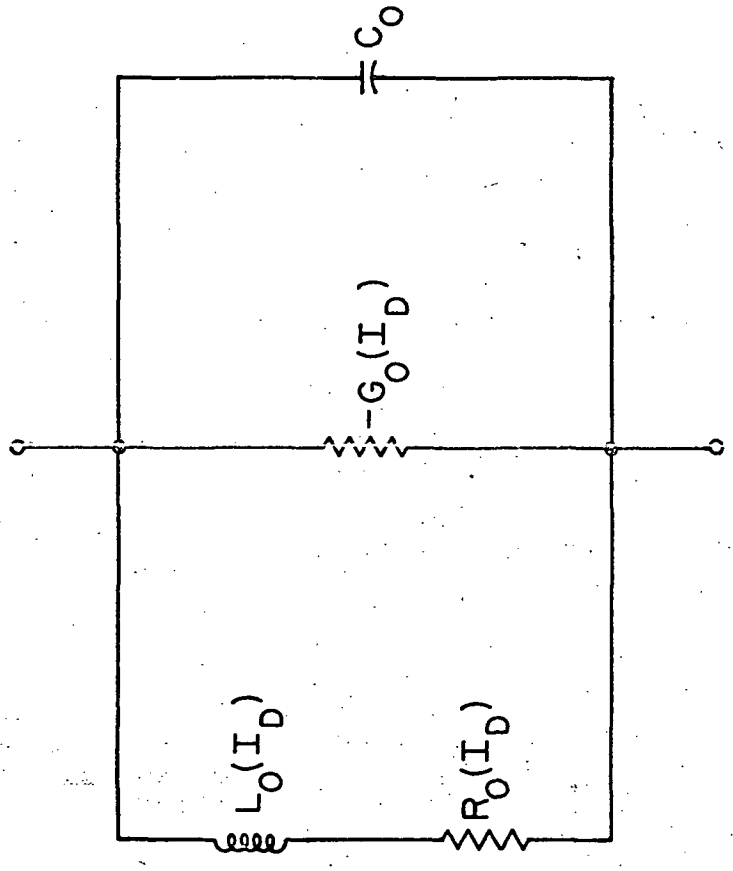
C_O
$-G_O(I_D)$
$L_O(I_D)$
$R_O(I_D)$

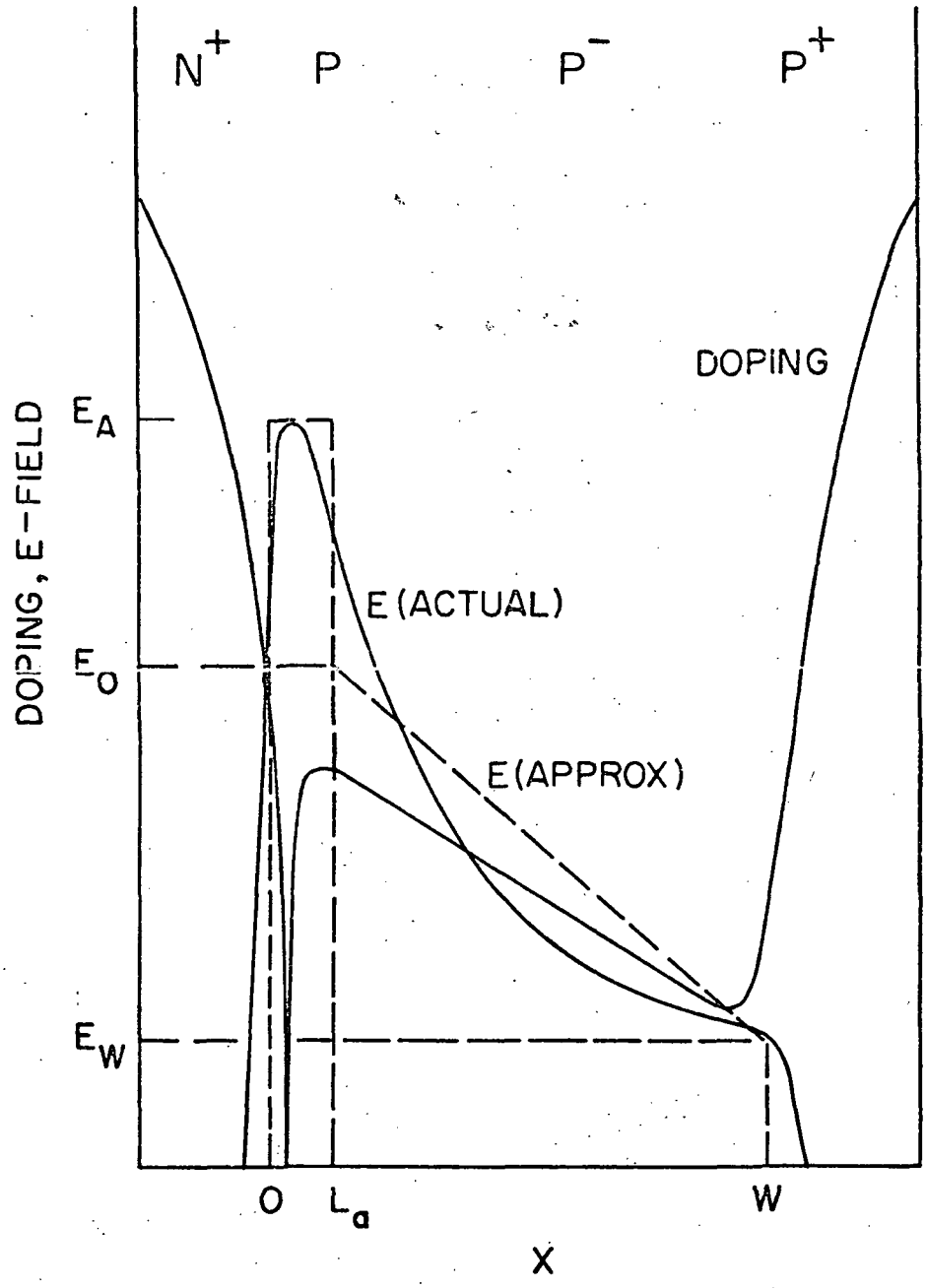

Fig 2
IEEE Trans. MTT

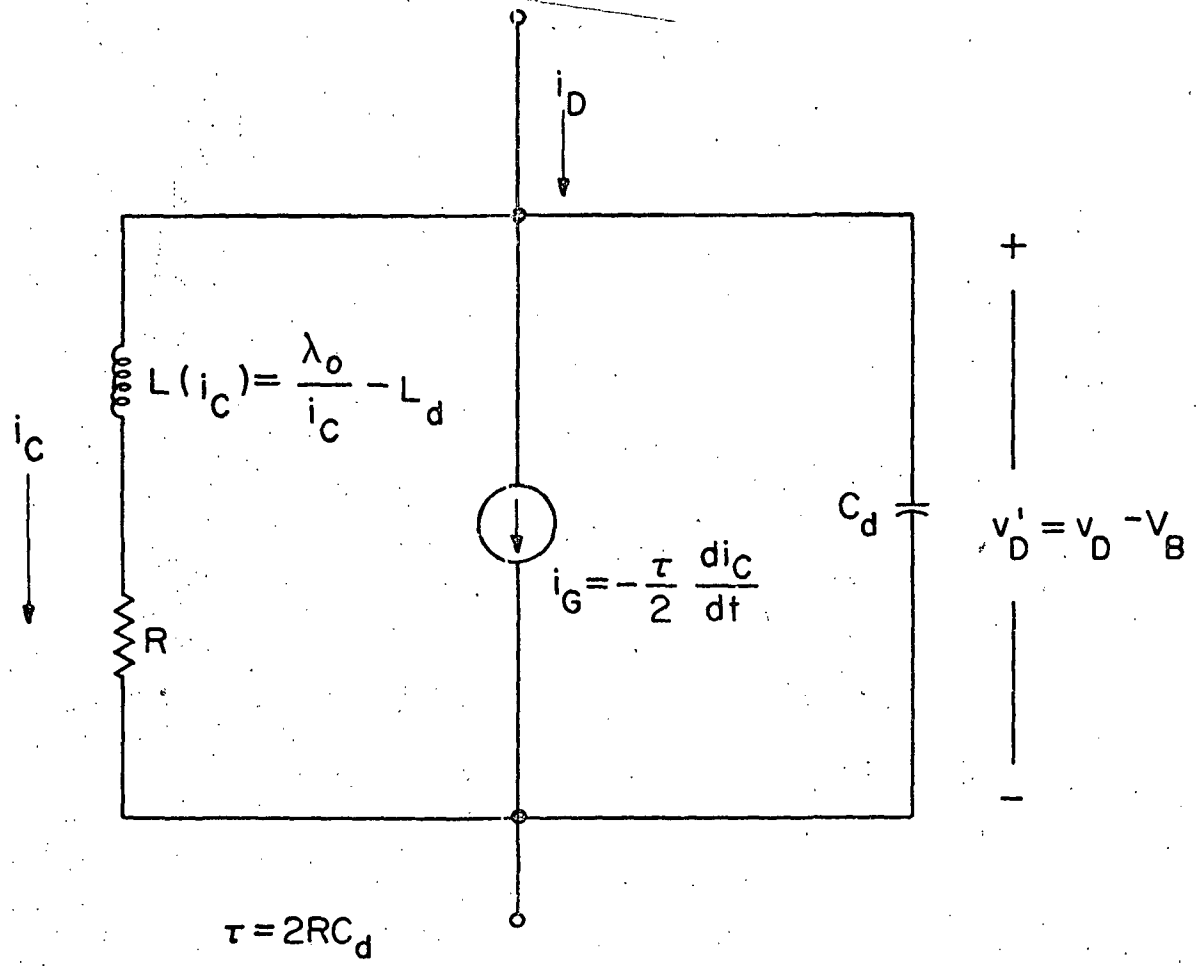
i_D
$L(i_C) = \frac{\lambda_o}{i_C} - L_d$
i_C
R
$i_G = -\frac{\tau}{2}\frac{di_C}{dt}$
C_d
+
$v_D' = v_D - V_B$
−
$\tau = 2RC_d$

Fig. 3

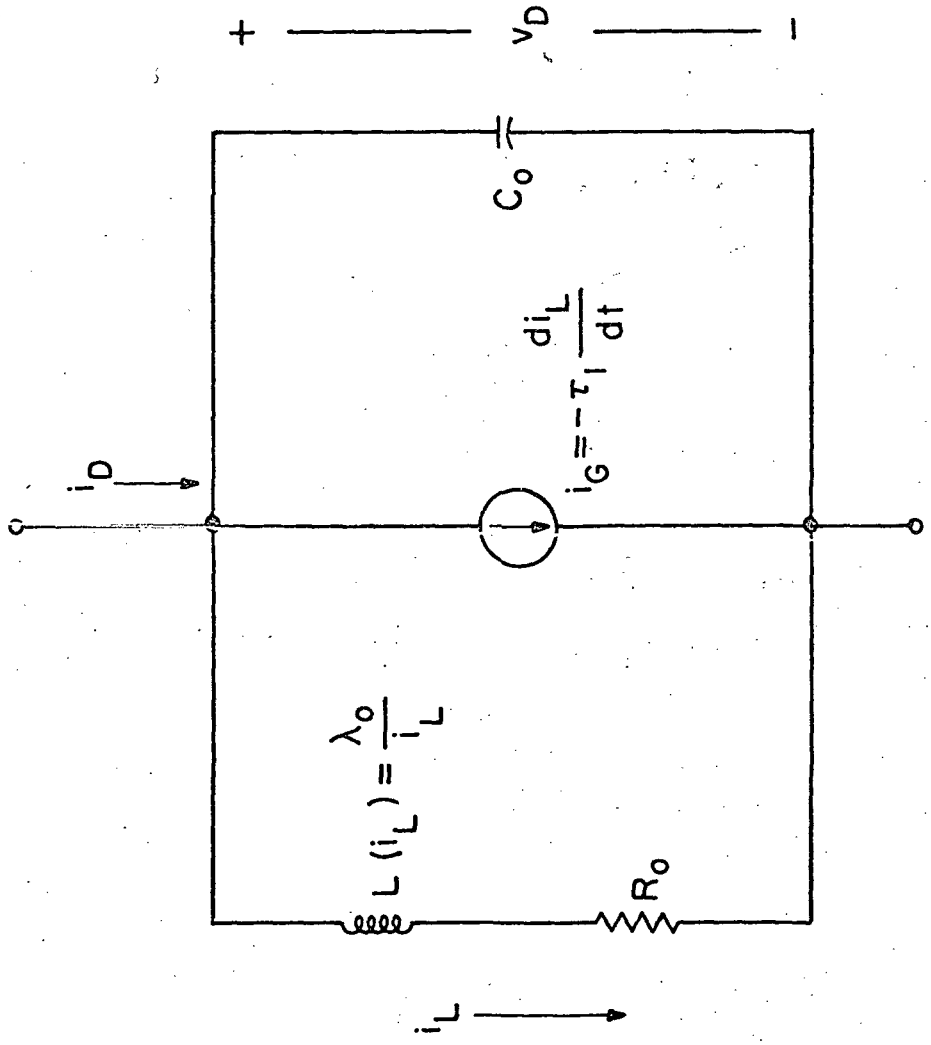
+
v_D
−
C_o
$i_G = -\tau_1 \frac{di_L}{dt}$
i_D
$L(i_L) = \frac{\lambda_o}{i_L}$
R_o
i_L

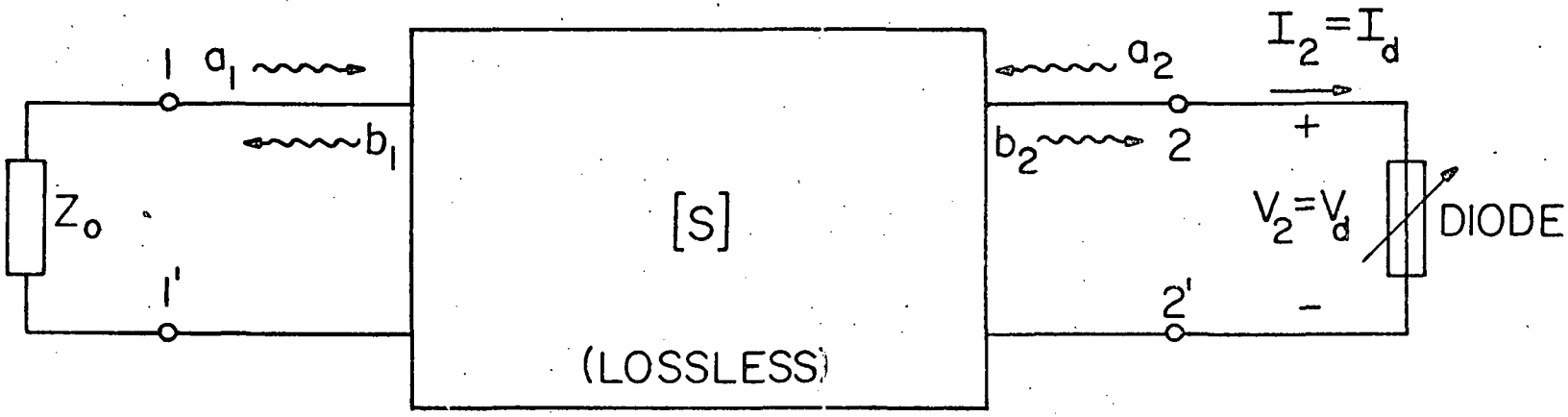

Fig. 5

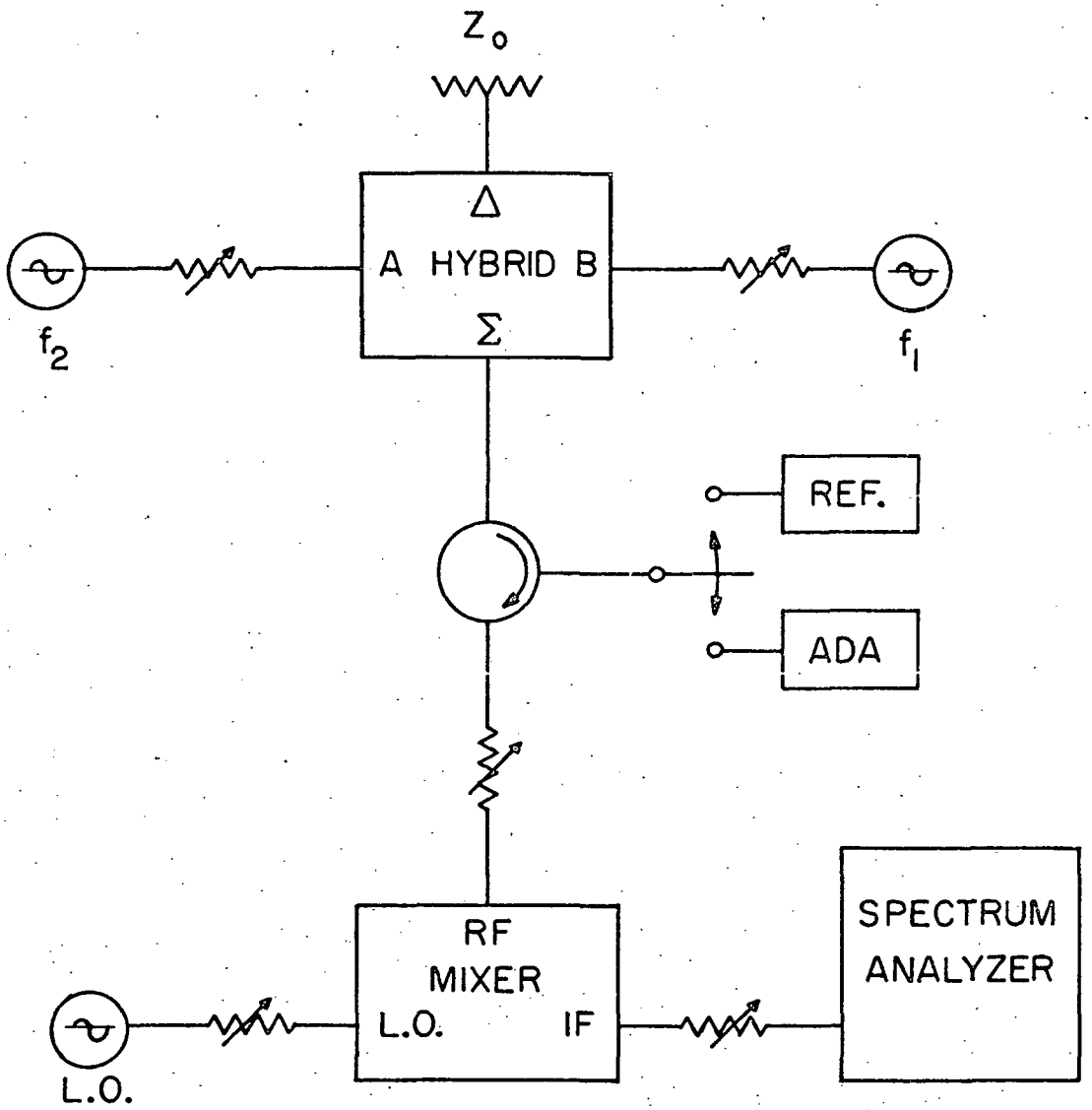
Z_o
Δ
A HYBRID B
Σ
f_2
f_1
REF.
ADA
RF
MIXER
L.O.
IF
L.O.
SPECTRUM
ANALYZER

6

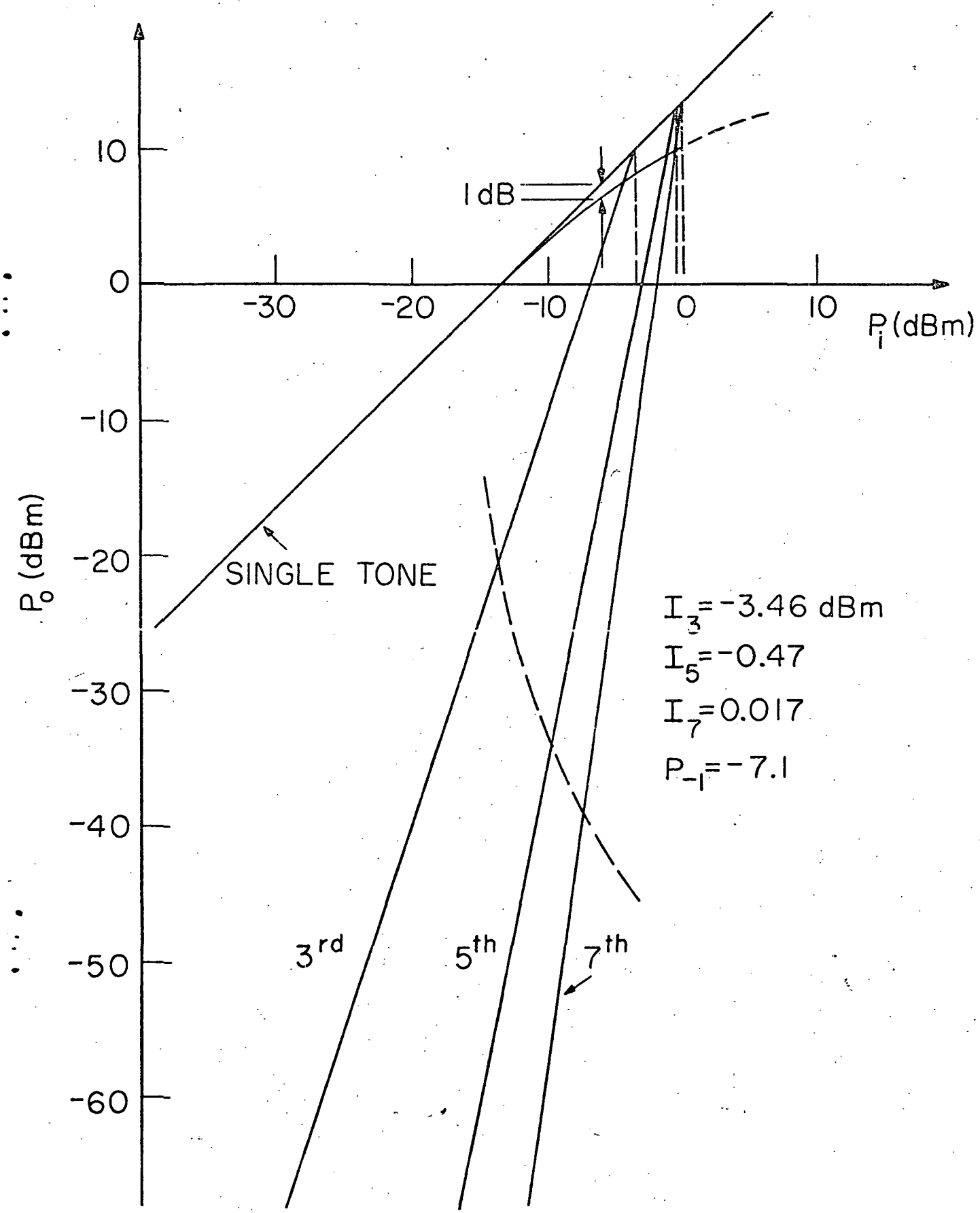
10
0
-10
-20
-30
-40
-50
-60
-30
-20
-10
0
10
P_i (dBm)
P_o (dBm)
1 dB
SINGLE TONE
I_3 = -3.46 dBm
I_5 = -0.47
I_7 = 0.017
P_{-1} = -7.1
3rd
5th
7th

Fig 7

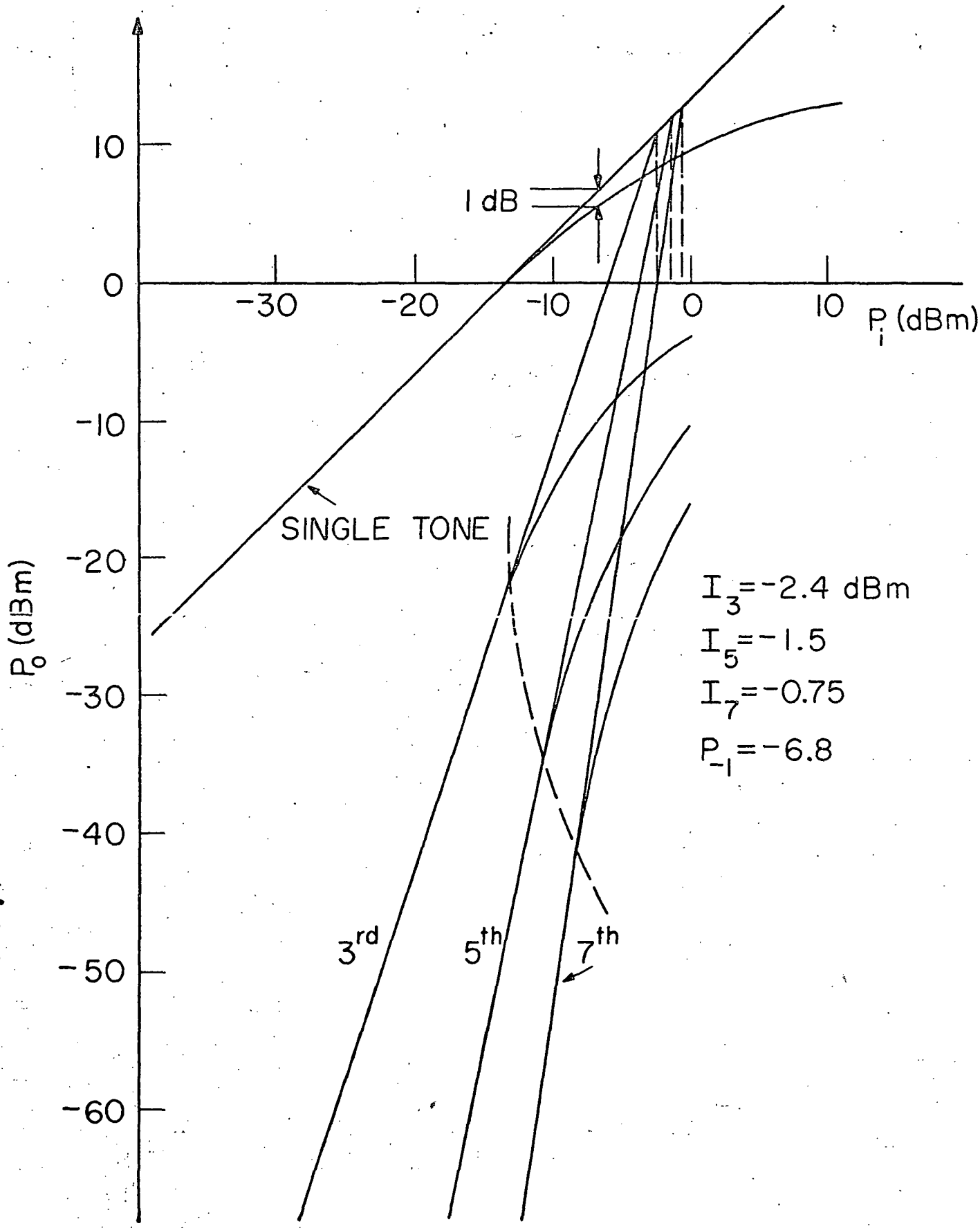
10
0
-10
-20
-30
-40
-50
-60
-30
-20
-10
0
10
P_i (dBm)
P_o (dBm)
1 dB
SINGLE TONE
I_3=-2.4 dBm
I_5=-1.5
I_7=-0.75
P_-1=-6.8
3rd
5th
7th

Fig. 8

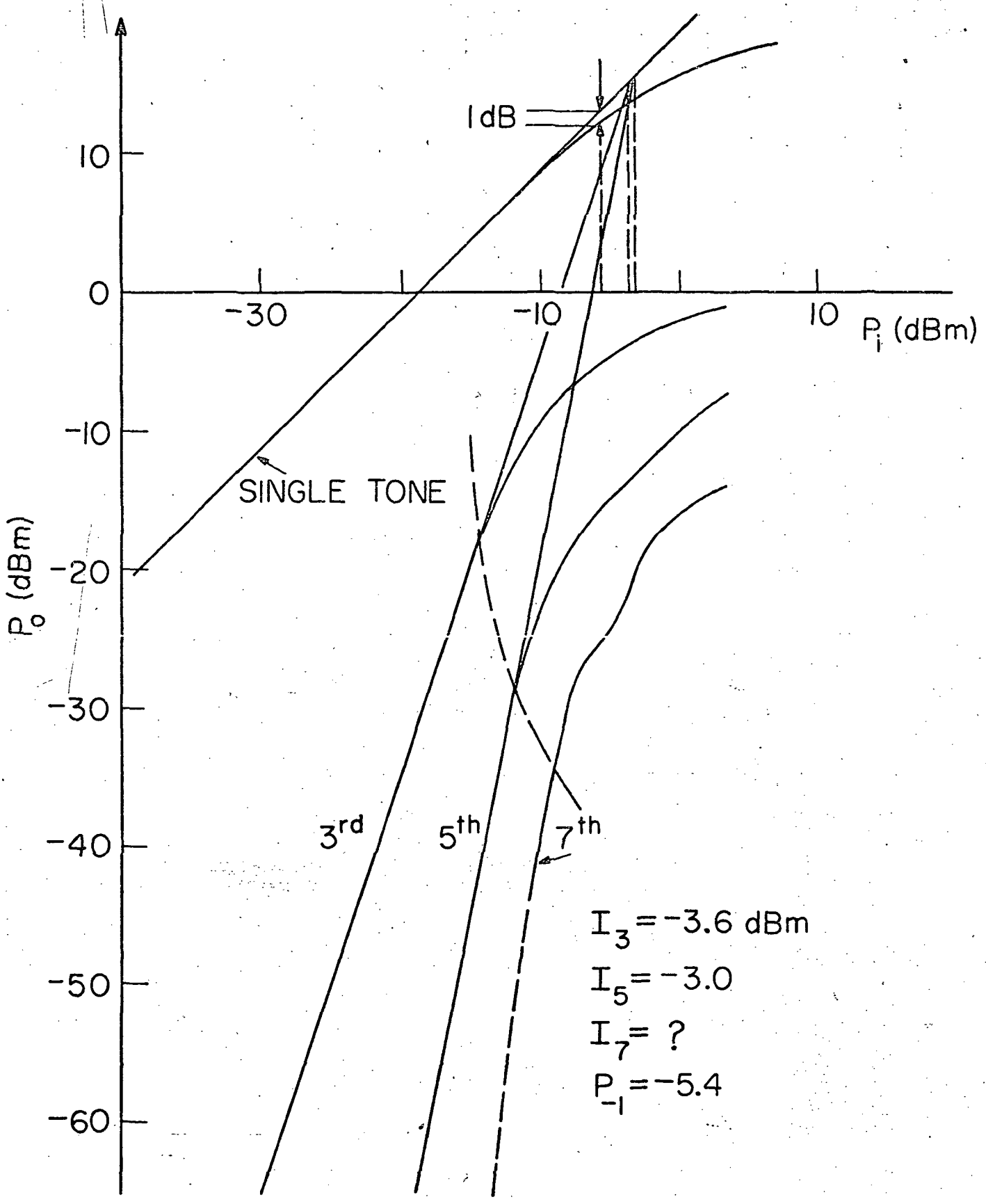
1dB
10
0
-30
-10
10
P_i (dBm)
-10
SINGLE TONE
P_o (dBm)
-20
-30
-40
-50
-60
3rd
5th
7th
I_3 = -3.6 dBm
I_5 = -3.0
I_7 = ?
P_{-1} = -5.4

Fig. 9

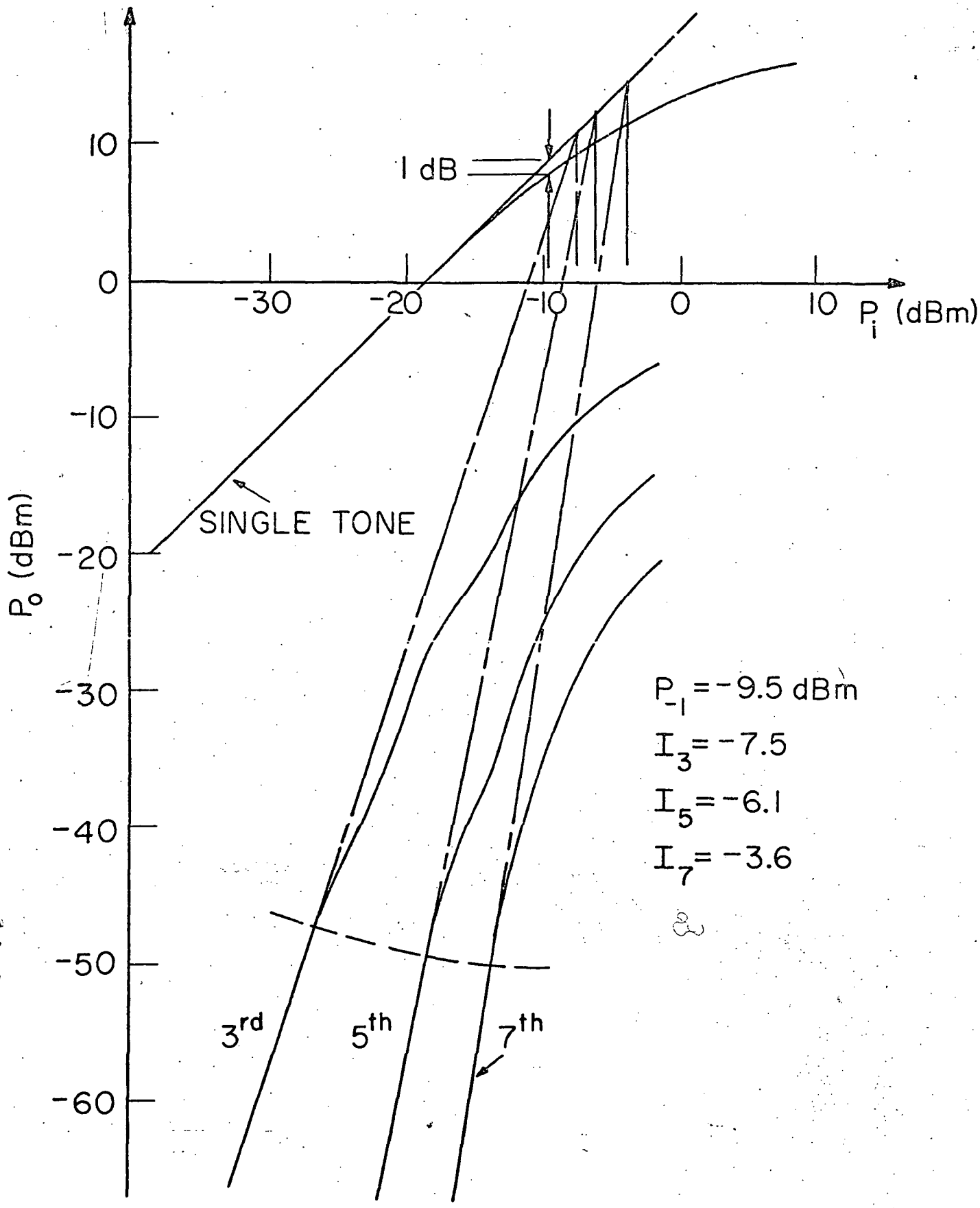
10
0
-10
-20
-30
-40
-50
-60
-30
-20
-10
0
10
P_i (dBm)
P_o (dBm)
1 dB
SINGLE TONE
3rd
5th
7th
$P_{-1} = -9.5$ dBm
$I_3 = -7.5$
$I_5 = -6.1$
$I_7 = -3.6$

Fig. 10